Fuel Cell Experiment

4/24/18

Alex Delafontaine, Jacob Kuebler, Luke Oluoch

Van Gogh

Main Author: Luke Oluoch

Abstract:

This lab was about approaching a fuel cell compartment and adjusting parameters that interacted with the fuel cell in order to maximize both power output of the compartment and efficiency. The fuel cell tested was a proton exchange membrane (PEM) fuel cell, constructed in a way that allows its compartments to be connected to a LabJack controlled with a LabView program. Controlled parameters included hydrogen gas flow rate, temperature, fan speed, relative humidity, and the external resistance of the circuit (the load). Two variables that appeared to most reliably increase the voltage output, efficiency, and power of the PEM were temperature and relative humidity. It was determined that to maximize both voltage and efficiency for our particular fuel cell, the temperature and the humidity would have to go as high as possible within our temperature range of 45 to 60°C (since going above that temperature would risk of damaging the structural integrity of the cell). While it would be preferable in regular circumstances to use lower temperatures, as lower temperatures would increase electrical conductivity, in this system, changing the temperature is linked to the relative humidity, so increasing it is the better option here. Changing load resistance

also had an effect on the system, as increased external resistance (load) led to increased efficiencies, but also led to decreased power. This behavior was consistent with the standard power performance curve expected for fuel cells. The calculated theoretical maximum voltage was 4.91 Volts and the theoretical maximum efficiency was 77.3%.

Introduction:

Proton Exchange Membrane (PEM) Fuel Cells are electrochemical devices that convert chemical energy harnessed from chemical reactions into electricity. These are especially useful because of their environmentally sustainability (fuel cells emit water as their product), and their relatively high chemical-to-electrical energy efficiency. However, unlike regular electrical cells, like batteries, these require a continuous supply of fuel in order to function. The PEM fuel cell used for testing utilized hydrogen gas for its fuel supply, meaning that it requires a source of hydrogen gas to function at all times it is running. The following reaction, using hydrogen gas takes place inside the fuel cell.

$$\text{Oxidation Half Reaction:} \quad 2H_2 + 4H_2O \rightarrow 4H_3O^+ + 4e^-$$

$$\text{Reduction Half Reaction:} \quad O_2 + 4H_3O^+ + 4e^- \rightarrow 6H_2O$$

$$\text{Net Reaction:} \quad 2H_2 + O_2 + 4H_2O \rightarrow 6H_2O$$

Equation 1. Oxidation Reaction, Reduction Reaction and Overall Reaction of a fuel cell.

At the anode, oxidation occurs. The fuel cell compartment takes in diatomic hydrogen gas and, using a catalyst, the hydrogen reacts with water to form hydronium ions, releasing electrons into a circuit. At the cathode, reduction occurs, the hydronium ions react with oxygen and electrons from the circuit to produce water. The energy from exergonic reaction can be converted into electrical energy by running the electrons separated through a circuit. The theoretical maximum voltage is proportional to the Gibbs Free energy of the reaction. The theoretical

maximum voltage is the voltage acquired under the assumption that all electrons transfer with no energy loss or outside effects whatsoever.

Eq. 2a

$$E_{ideal} = -\frac{\Delta G}{NF}$$

$E_{ideal} = Ideal\ Voltage\ Produced\ By\ Battery\ at\ STP$
$\Delta G = Gibbs\ Free\ Energy\ of\ Fuel\ Cell\ Reaction\ at\ STP$
$N = Number\ of\ Electrons\ Transfered$
$F = Faradays\ Constant$

Eq. 2b

$$\varepsilon = \frac{E}{E_{ideal}}$$

$\varepsilon = Efficiency$
$E = Measured\ Voltage$

Equation 2a, 2b. Equations used to calculate efficiency in the fuel cell stack.[3]

The Fuel Cell has components called bipolar plates necessary for electron transfer. These are the structures between the two electrodes that give the fuel cell its shape and allow the electrons to transfer between the electrodes. They allow for multiple fuel cells to be stacked on top of each other in order to form a series and build up more total voltage. Additionally, they provide pathways that allow the hydrogen gas and the oxygen gas to flow out different ways, enabling unreacted hydrogen to be recycled and water vapor that is formed to be removed from the system. Well designed bipolar plates will have the right thermal and electrical conductivities to ensure that heat is transferred properly and that the electrons are not hindered by the system(Yeetsorn, 2011).

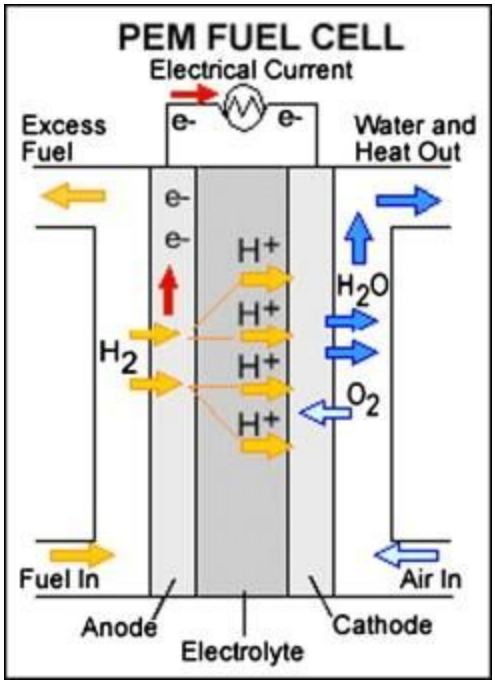

Fig. 1. Basic set-up of a PEM Fuel Cell

Because the fuel cell system that was used contained four individual fuel cells aligned in series, multiple voltages could be detected in the cell as shown by the following diagram of the electrical circuit, figure 2:

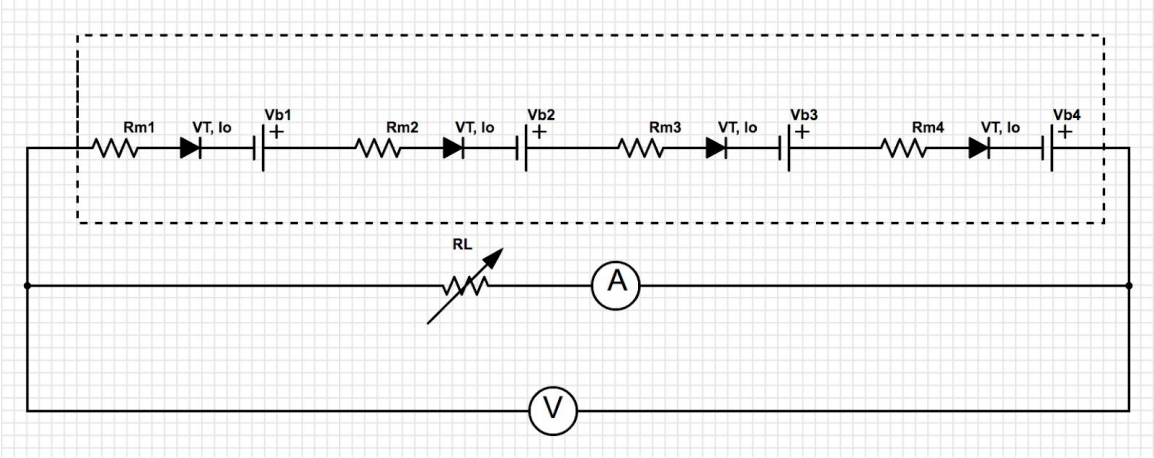

Fig. 2. Electrical diagram of Fuel Cell

In figure 2, V_n is the measured battery voltage in series, $V_{b,n}$ is the fuel cell battery voltage, $V_{T,n}$ is the diode threshold voltage, i is the current, $I_{o,n}$ is the diode saturation current, and $R_{m,n}$ is the internal resistance. In all cases, *n* is used to indicate the fuel cell number.

Physically, the measured battery voltage, $V_{n.i}$, is the voltage that the individual cell is giving out and that differs from the battery voltage, $V_{b,i}$. The measured voltage will always be lower than the battery voltage, as the battery voltage is the maximum voltage achievable in the cell if the effects of the current and resistance are negligible. The measured voltage is affected by the diode saturation current, $I_{o,i}$, which is the current that is formed by a minority of electrons flowing in the opposite direction due to the chance of them entering the space charge region. Threshold voltage, $V_{T,i}$, is the minimum voltage that is required for conduction (flow of electrons through the layer) to begin occurring. Internal resistance is the physical resistance of mass transfer in the electrolyte that the individual fuel cell exhibits. This is a characteristic of the structure and composition of that cell. These all play their part in measuring the overall voltage of each cell, but each cell does not end up having equivalent voltages. There are discrepancies between the cells. A possible reason for this is that the fuel cells could have different resistances in each interface. This happens because catalyst poisoning can alter the threshold voltage or from delamination making differences between electrolyte-electrode interface alter the saturation current. Another reason could be

the electrolyte in each cell having a different resistance, caused by each cell having varying degrees of water content from the reaction. This would change the physical conductivities and lead to each cell having differing internal resistances. The individual voltages could also be different from each cell having slightly different hydrogen flow rates or from flooding occurring (Bezinger, 2005).

$$V_n = V_{b,n} - V_{T,n} \ln\left(1 + \frac{i}{I_{o,n}}\right) - iR_{m,n}$$

Eq. 3. Voltage Model Equation Based on Internal Fuel Cell Parameters[1]

Because the fuel cells are in a series, the current flowing through each cell is identical. However, each cell will have different internal resistances, threshold voltages, saturation currents and produced voltages for the same current output voltages. It is important to measure the voltages of each cell and the total voltage because revelations can come to light of why certain conditions cause anomalies in data.

Another important concept is that of the polarization curve. The polarization curve is used to describe the best electrical boundaries within which to operate a fuel cell. It can help describe what is happening on a chemical and physical level within the cell. The diagram below is an example of what one should look like.

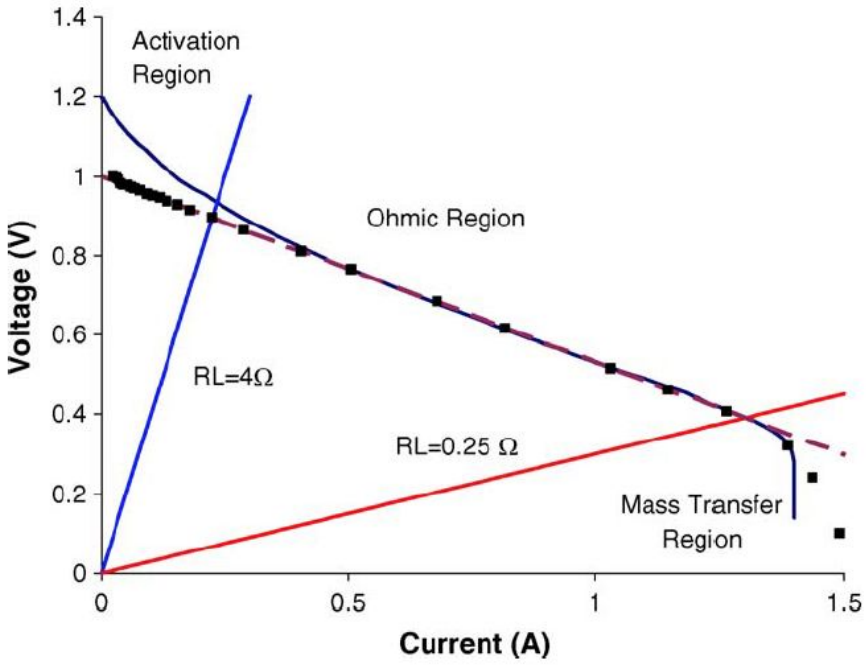

Fig. 3. Standard Polarization Curve of a Fuel Cell[1]

Figure 3. shows the relationship between the current flowing through and the output voltage of a fuel cell. With high currents, i.e., low external resistance, the fuel cell is limited by the rate of diffusion to the electrodes and electrolytes. The region where diffusion limits the fuel cell is aptly named the mass transfer region. At very low currents, i.e., high external resistance, the fuel cell has trouble overcoming the activation energy. This region is known as the activation region. The goldilocks-zone of this diagram lies right in the middle, as the linear trend suggests that the only factors affecting current and voltage are each other, which is the ideal situation.

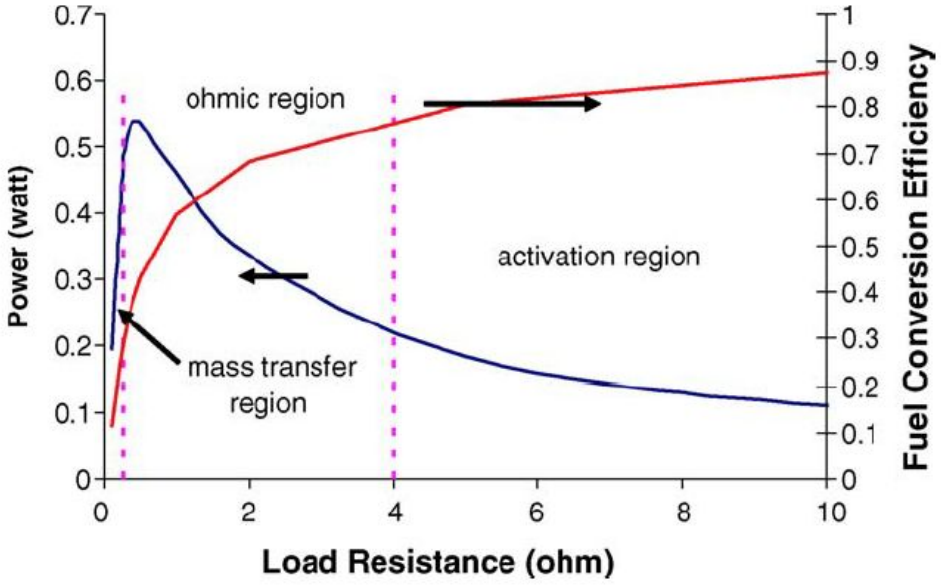

Fig. 4. Power Performance Curve of a Fuel Cell[1]

Alternatively, the load resistance can be plotted against power and efficiency. As is shown here a mass transfer region exists at low resistances and the activation region exists at high resistances. This makes sense with what was determined earlier, as resistance will behave inversely to current. It's also important to compare how power and efficiency differ in this area. Essentially what it shows is that it is impossible to maximize both power and efficiency, so it is important to determine which is the one that is desired when trying to build the perfect system.

Lastly, it is important to reiterate the potential that lies within fuel cells as an alternative method of harvesting/storing electrical energy. Hydrogen gas is a cleaner fuel in that it only produces water when reacted. Hydrogen gas can be made from processes that may be have low environmental impact like electrolysis, which can be performed efficiently near sources of water, using sunlight as energy, while a

portion of hydrogen used in fuel cells today is also produced by the petroleum industry. The biggest difficulty with using hydrogen gas is that it is difficult to store, meaning that in many cases fuel cells must be localized to where hydrogen gas is being produced. The high efficiency that is possible in fuel cells when there is ready access to hydrogen can used to replace our current, outdated electrical infrastructures. This field of study is an essential one to study as the energy industry moves into the future.

Equipment:

In this lab, a PEM Fuel Cell built by Thor Olsen was used.

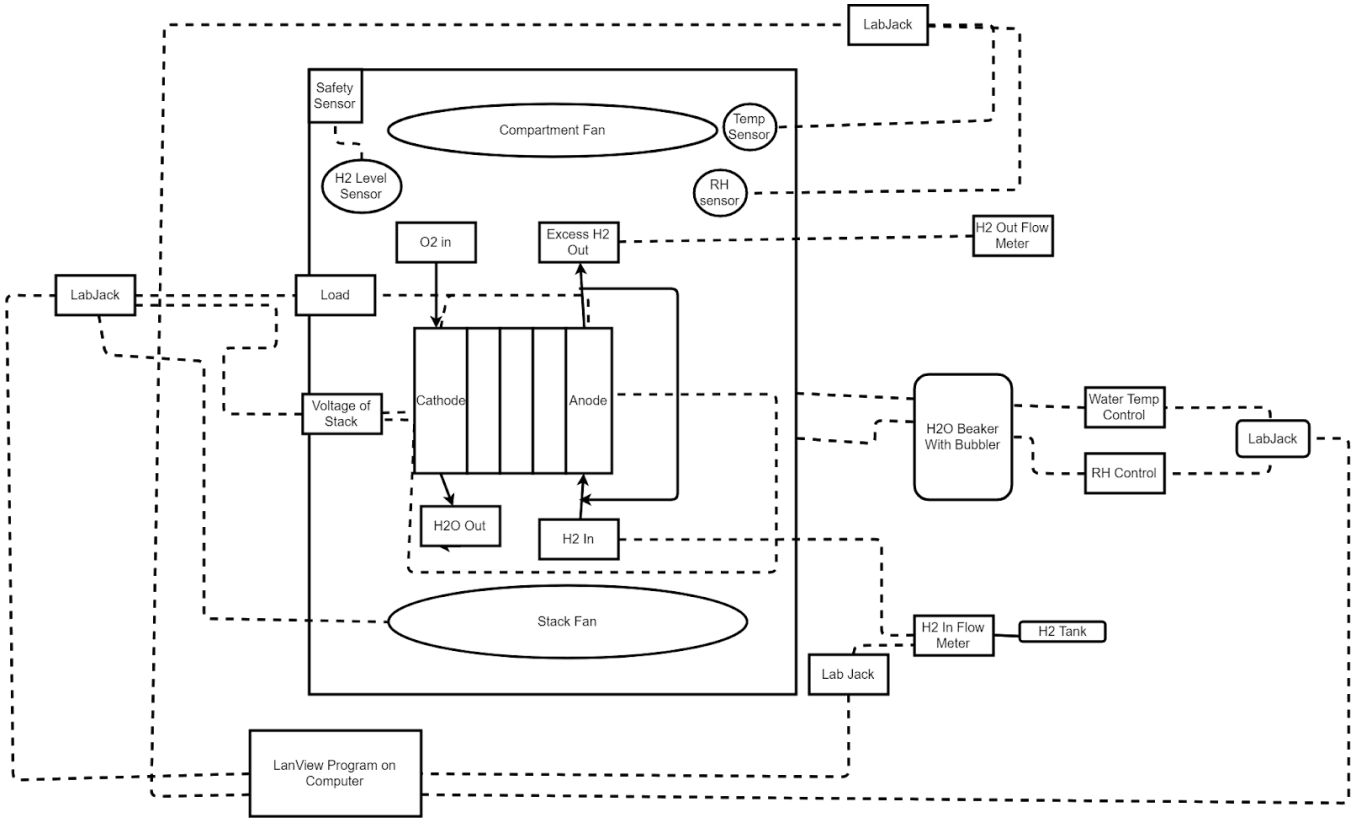

Fig. 5. PID of the Fuel Cell.

It was used in conjunction with National Instruments LabView Software and their accompanying physical component, the LabJack U12, shown in the figure below.

Fig. 6. LabJack U12

The fuel cell was stored within a box, which maintained a controlled environment for important fuel cell parameters (temperature, relative humidity and hydrogen flow rate).

Experimental Procedure:

Setup Procedure:

Before turning on the fuel cell, make sure to turn on the air flow and set the air flow rate to 4 GPM. This is to prevent high mole fractions of hydrogen gas from forming. The air should be kept at this relatively high flow rate compared to the

hydrogen flow rate in order to make sure the mole fraction of hydrogen in the fuel cell never exceeds 4%, since hydrogen will combust at high molar fractions in air.

The humidifier within the fuel cell box, requires water to control the relative humidity of the system, so it must be filled with a proper amount of deionized water before the fuel cell is turned on.

To start the fuel cell, along with the measurement equipment and computer system, the hydrogen generator must be switched on, which produces hydrogen gas that fuels the PEM. When the hydrogen pressure in the generator reaches 15 PSIG, the shut-off valve can be opened to let hydrogen into the fuel cell box. The initial load and the total hydrogen flow in the program are both set to zero initially, and the temperature is set to around room temperature, 25°C.

Experimental Procedure:

To analyze the correlations between controlled parameters and power or efficiency, certain parameters were adjusted while everything else remained constant. The controlled parameters were humidity, temperature change, load (external resistance), and excess hydrogen flow that passes through the cells. Each of these parameters could be controlled through a LabView program connected to the fuel cells. Special care should be taken when changing temperature, since there are two temperatures that can be controlled: the water temperature of the humidifier and the temperature of the fuel cell box must both be set to the desired temperature.

Test 1. Humidity Test:

First, humidity was changed from 30% to 60% in increments of 5% while temperature was kept at a constant 30°C, fan speed at 99%, and hydrogen flow rate in kept at 30 mL/min . The humidity was then decreased from 60% to 30%. The efficiency and power output were recorded.

Test 2. Temperature Test:

Next, temperature was changed within the range of 25°C to 60°C, while relative humidity was kept at around 40% (this was difficult to control since keeping humidity at 40% while raising temperature sometimes can exceed the demands of the humidifier), fan speed was kept at 100%, and hydrogen flow rate were kept constant at 45 mL/min. The temperature was increased continuously in this test. The efficiency and power output were recorded.

Test 3. Temperature/Humidity Test:

After gathering data from the individual humidity and temperature tests, we attempted to perform a 2x2 factorial analysis of temperature and humidity. In this test, two parameters were varied, temperature and humidity, with flow rate remaining constant. The load resistance took the form of a square wave, when the resistance was high (92 Ohms) the current was low (0.05 A), letting the fuel cells "rest". Data was taken from the portion of the square wave where the resistance was low (5 Ohms), meaning the current was reasonably high (0.5 A). Temperature was

held constant in the range of 45 to 60 C at increments of 2.5 C. At each temperature increment, the humidity was maxed out then brought down to around 25 RH. The results were taken into JMP and a 2x2 factorial analysis of the effects of humidity and temperature on efficiency and power was performed.

Test 4. Hydrogen Flow Rate Test:

Next, hydrogen flow rate was changed from 20 mL/min to 40 mL/min in increments of 5 mL/min while relative humidity was kept at 55%, temperature was kept at 40°C, and fan speed at 99%.

Test 5. Load Resistance Test:

The load resistance was changed so that a range of currents from nearly 0 to 2 A were achieved. The hydrogen flow rate was held constant around 90 mL/min, the temperature was held at 60 C and the relative humidity was 30%

All the data was recorded and graphed. The data was subsequently modeled and interpreted through JMP, Microsoft Excel, and Python.

Results/Discussion:

Test 1. Humidity Effects on Power and Efficiency:

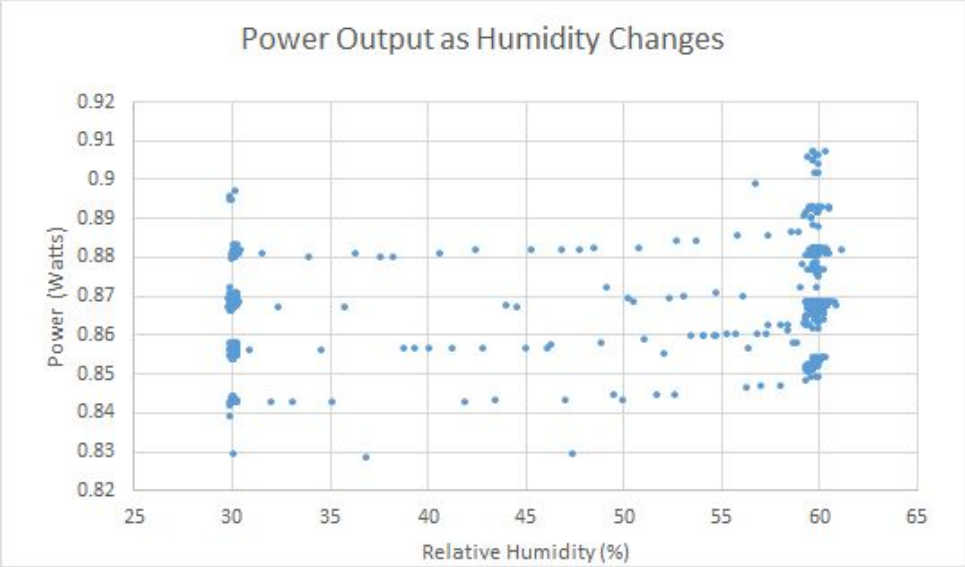

Fig. 7. Experimental Data for Power vs. Humidity

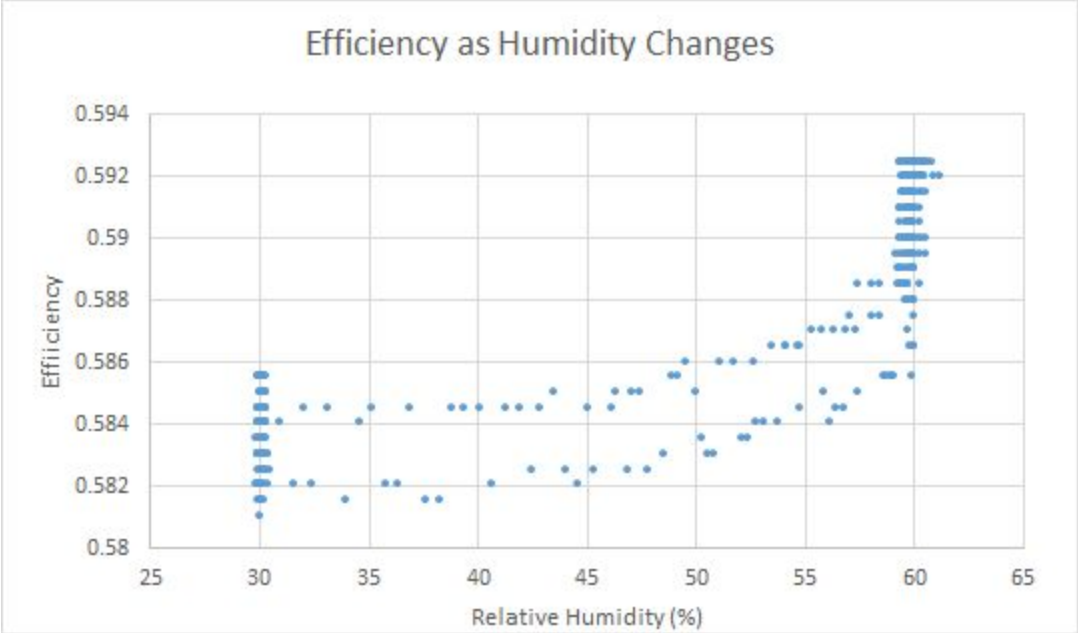

Fig. 8. Experimental Data for Efficiency vs. Humidity

Figures 7 and 8 compared relative humidity with power output and efficiency and a positive correlation can be observed. This run was done under a constant load, i.e., external resistance, and at a constant temperature. Increasing relative humidity will increase the partial pressure of water. An increase in the partial pressure of water facilitates the transport of ions through the electrolyte as the oxidation reaction requires water to be converted into hydronium ions that diffuse across the electrolyte. Since the voltage in the normal operating region, the ohmic region, is controlled largely by the resistance in the electrolyte, decreasing the resistance will increase the voltage output of the system for a specific current.

Test 2. Temperature Effects on Power and Efficiency:

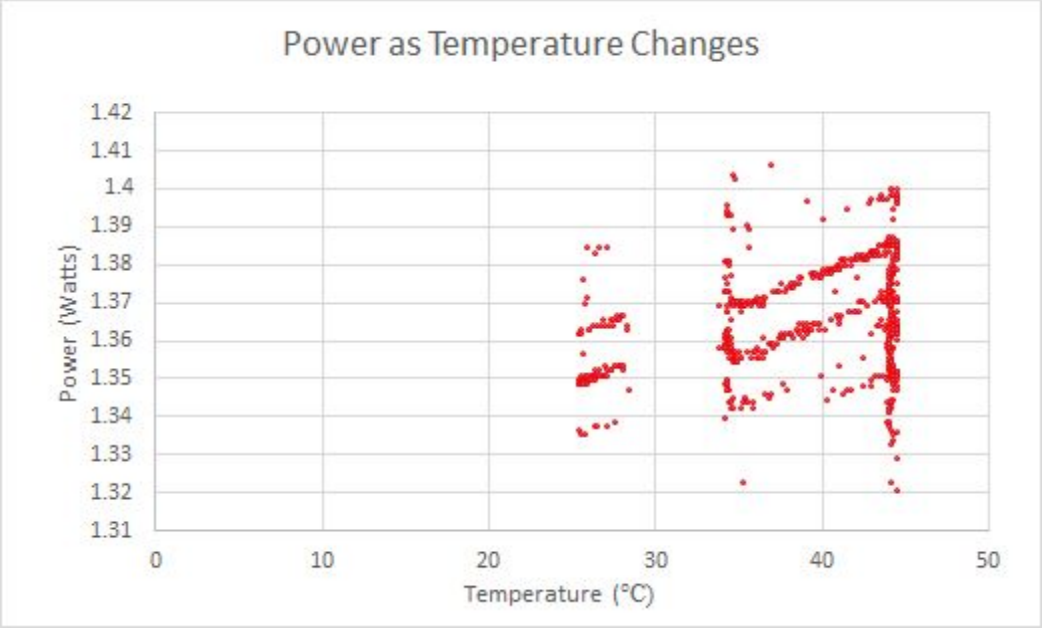

Fig. 9. Experimental Data for Power vs. Temperature

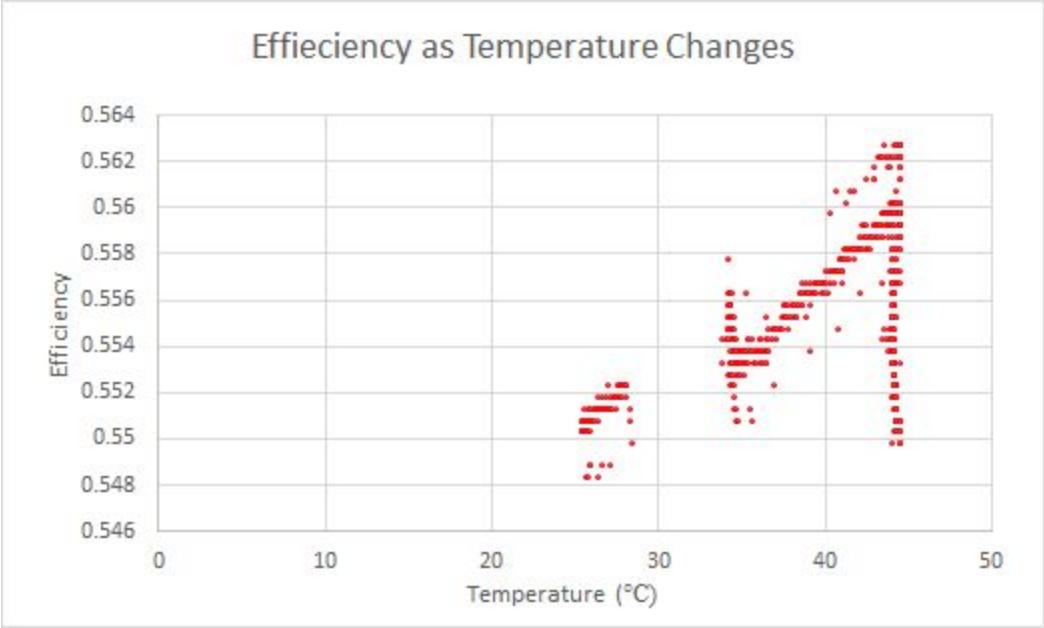

Fig. 10. Experimental Data for Efficiency vs. Temperature

In figures 9 and 10 it is shown that as temperature increases within our range of data, a positive trend was observed for both efficiency and power (at a constant hydrogen flow rate and relative humidity). There is a gap in measured data between the 29° and 34° because the fan speed to the fuel cell stack was inconsistent for those data points. One possible explanation for the positive trend observed in both power and efficiency is that since relative humidity was constant, the partial pressure of water increased as temperature was increased. This would lead to a similar increase in power and efficiency to what occurs when relative humidity is increased. However, it is likely that the temperature may affect other aspects of the fuel cell other than the partial pressure of hydrogen introduced, since

the effect of temperature on power and efficiency appears to follow a more linear trend than the effect of relative humidity on power and efficiency.

Test 3. Humidity/Temperature Analysis:

After determining that temperature and humidity affect temperature, an experiment was designed that tested both relative humidity and temperature within 2x2 factorial design. While the temperature and humidity analysis were valid at certain conditions, the model could not be extended to a range of temperatures. The analysis performed for this test sought to examine a broader range of humidity and temperature data than previous tests could. In addition, this analysis sought to identify if there were interaction effects between humidity and temperature, but they were deemed insignificant, with a P-Value much greater than 0.05, and the factorial analysis was redone without testing for interactions.

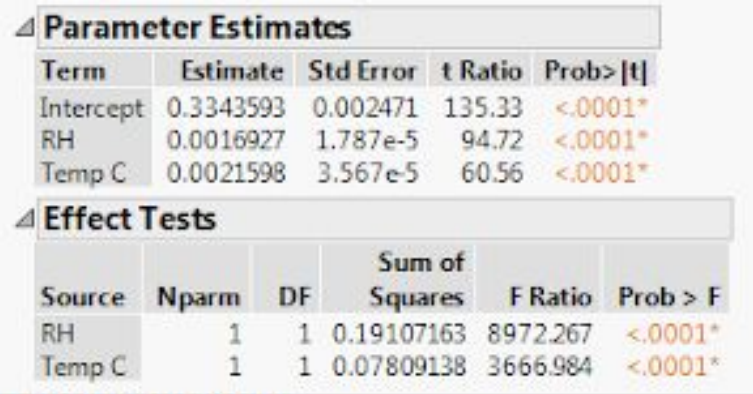

Parameter Estimates

Term	Estimate	Std Error	t Ratio	Prob>|t|
Intercept	0.3343593	0.002471	135.33	<.0001*
RH	0.0016927	1.787e-5	94.72	<.0001*
Temp C	0.0021598	3.567e-5	60.56	<.0001*

Effect Tests

Source	Nparm	DF	Sum of Squares	F Ratio	Prob > F
RH	1	1	0.19107163	8972.267	<.0001*
Temp C	1	1	0.07809138	3666.984	<.0001*

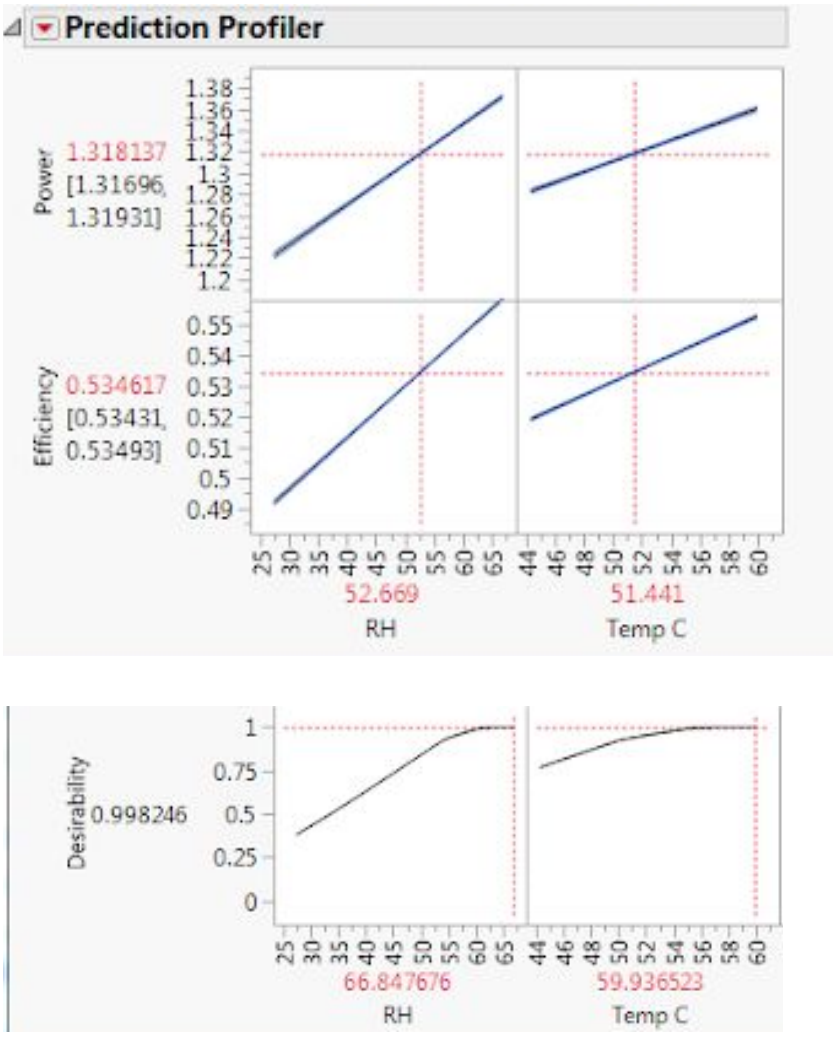

Fig. 11. JMP Analysis of combined Relative Humidity and Temperature effects on Power and Efficiency

Figure 11. shows that as both Temperature and Humidity were increased, the power and efficiency rose as well. We set the desirability to be based on maximizing both efficiency and power, so the desirability is highest at the highest temperature and humidity in our range of data. What this does not take into account however is flooding, when humidity is so high that water vapor starts condensing on the cathode side of the fuel cell and inhibits mass transfer in the electrolyte. We were

unable to go up to such a high level of humidity in the experiment, since our equipment could not evaporate water at a fast enough rate to maintain high relative humidity. It is entirely possible that outside the range of humidity and temperatures we tested that humidity and temperature have an inverse effect on power and efficiency. Further testing would look to examine higher or lower temperatures and relative humidities.

Test 4. Hydrogen Flow Rate:

The excess flow rate of hydrogen gas was varied in order to identify if there was any correlation between hydrogen flow rate in to power or efficiency. We performed analysis in JMP in order to tell if the change in hydrogen flow affected our system.

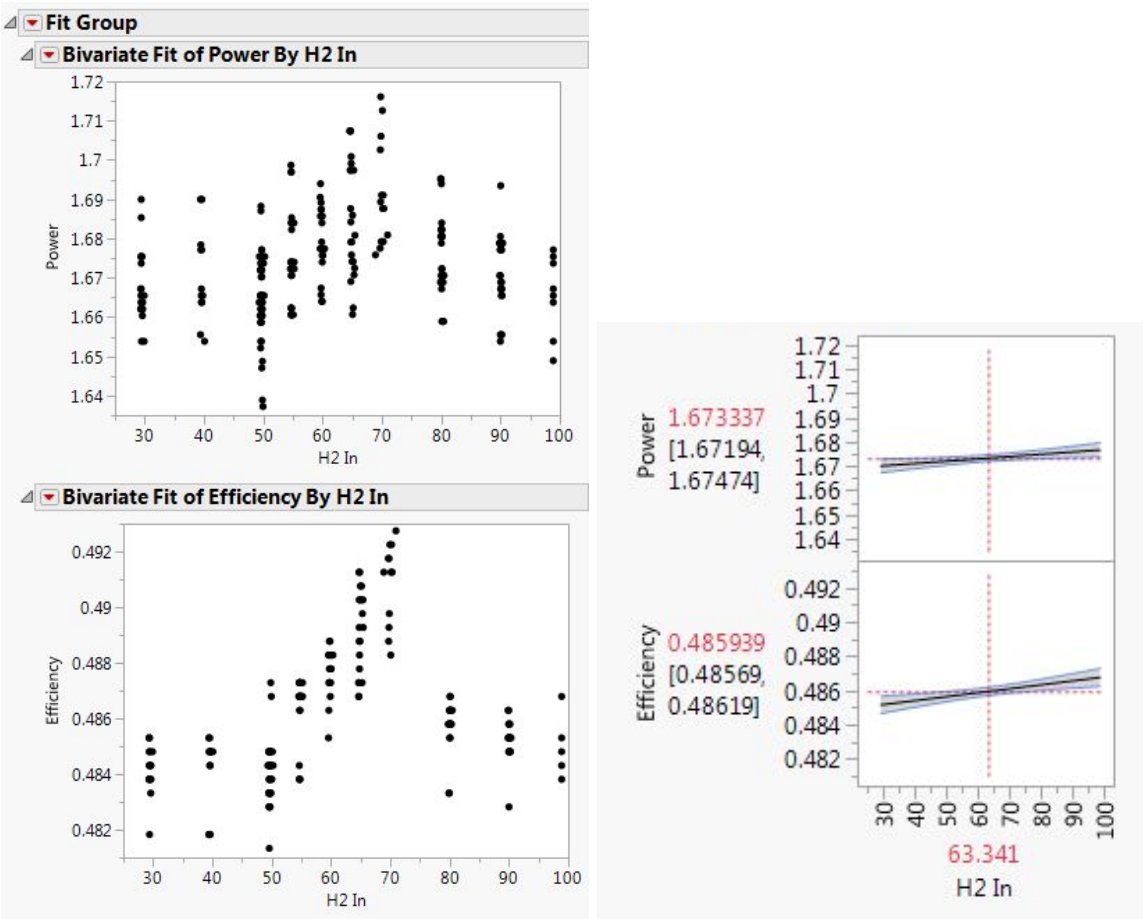

Parameter Estimates

Term	Estimate	Std Error	t Ratio	Prob>|t|
Intercept	1.6672899	0.002477	673.17	<.0001*
H2 In	9.5474e-5	3.746e-5	2.55	0.0113*

Fig. 12. JMP analysis of Hydrogen Flow Rate effects on Power and Efficiency

In figure 12 we show the correlation we derived by changing the hydrogen flow rate from 30 mL/min to 100 mL/min. In this analysis we obtained a probability that the

hydrogen flow rate affects power and efficiency of P-Value = 0.0113. We are looking for P-Values much less than 0.05, which we did not obtain with our P-Value of 0.0113. We do observe a slight increase in power and efficiency as we increase hydrogen flow rate, but we cannot say that the results are significant enough for our criteria. It was determined that hydrogen flow was not a variable that majorly affected the cell. This could be because at all times, the excess was kept constant, so overall the cell could tell no difference between any change of hydrogen.

Test 5. Load Resistance Effects on Efficiency and Power:

With changing current, we observed the following data on both efficiency and power.

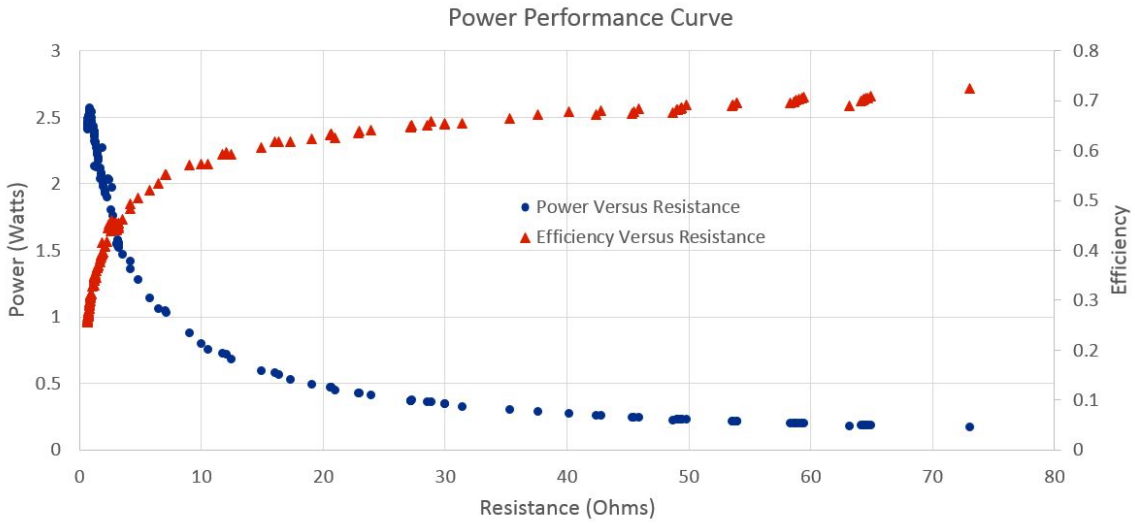

Fig. 13. Power Performance Curve based on Experimental Data

This experimentally derived power performance curves looks almost identical to the power performance curve found in literature (fig. 4). Analysis of the power performance curve was done in JMP, shown on figure 14 below.

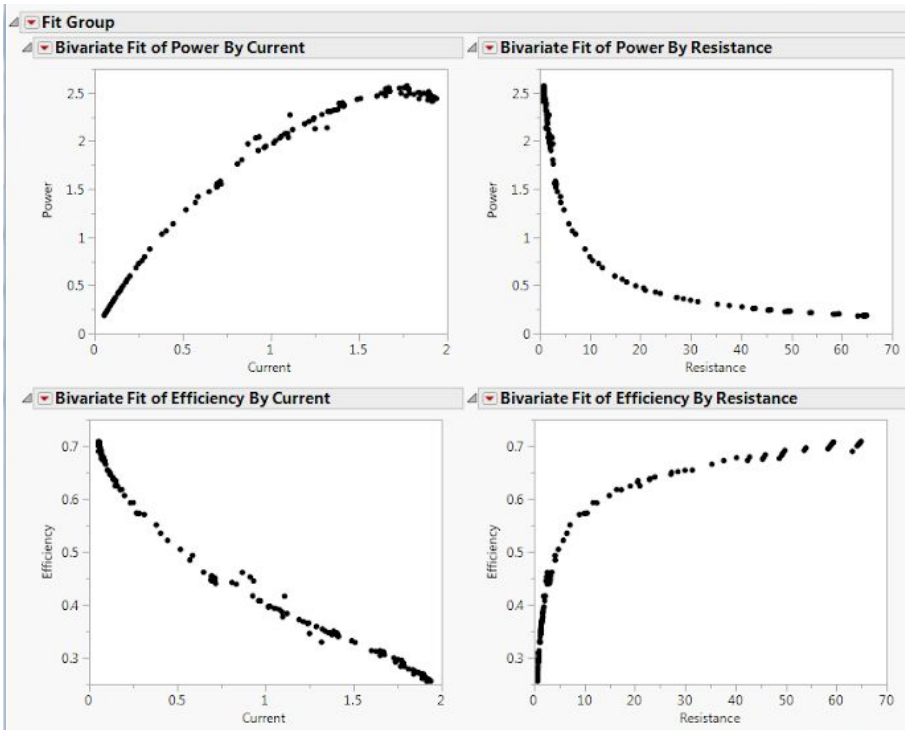

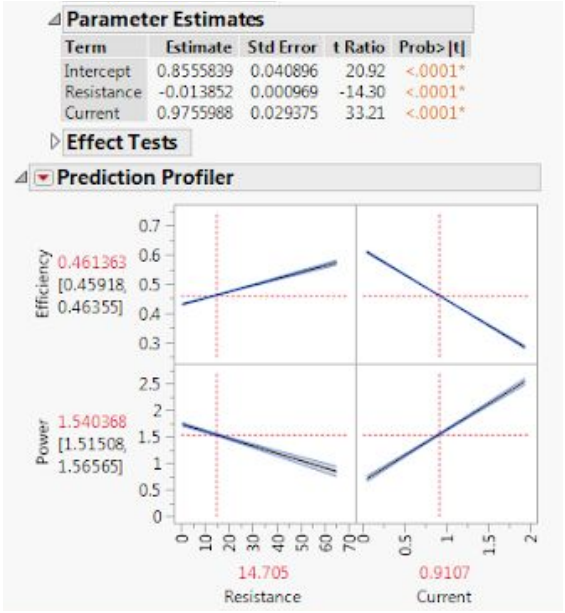

Fig. 14. JMP Analysis of Resistance and Current Effects on Power and Efficiency

The prediction profiler shows a positive trend that correlates resistance and efficiency. Similarly, current and power show a positive correlation. Current, when

stacked against efficiency, shows a negative correlation. The same can be seen from the prediction profile of resistance and power. This shows that both power and efficiency cannot be simultaneously maximized by controlling current and resistance. In terms of power, increasing the resistance creates a power drop, yet increasing current increases power. The inverse of this can be seen for efficiency, as when resistance increases, efficiency increases as well. However, increasing current makes the efficiency decrease. Together, the bivariate fits for power and efficiency with respect to current and resistance resemble the power performance curve.

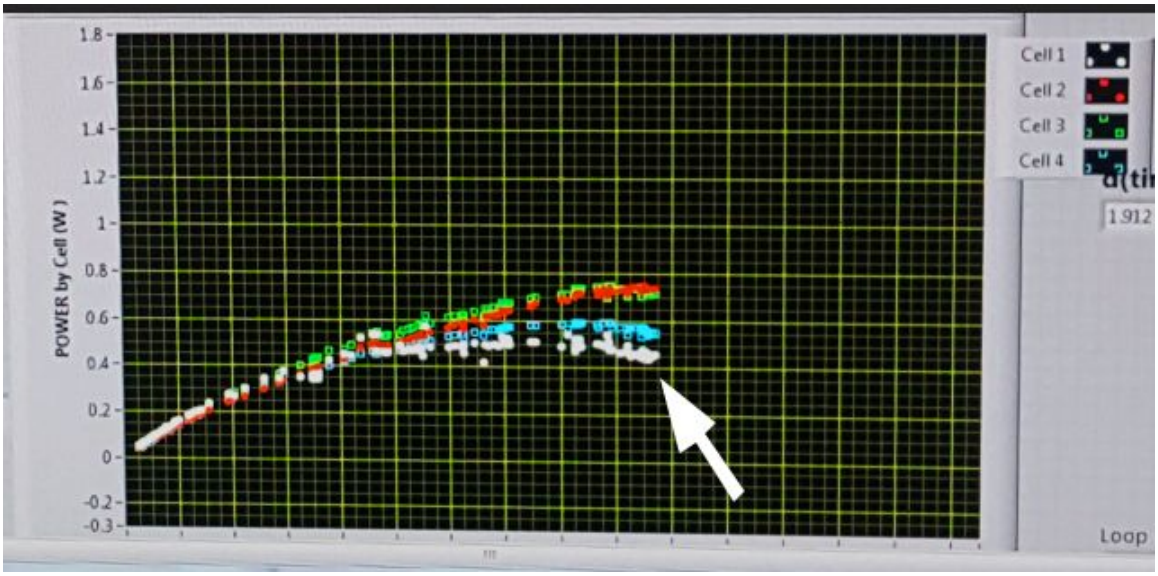

Current (A)

Fig. 15. Photo of LabView Program Running Indicating the Weakest Fuel Cell

Additionally, as shown by figure 15, it was observed during the experiment that the first cell (white) in the stack and the last cell in the stack began to fail at high load (high currents) before the middle two cells in the stack (red and green). That is, at higher currents, the power output that could be achieved by the first and

last cells in the stack was limited, while the power output from the middle two cells was much higher. One way to understand what may be occuring in cells that perform differently from one another is to regress the voltages of each individual cell with respect to current to determine parameters in Eq 3 (shown/labeled above):

$$V_n = V_{b,n} - V_{T,n} \ln\left(1 + \frac{i}{I_{o,n}}\right) - iR_{m,n}$$

Where Vn is the measured voltage, the dependent variable, and i is the current, the independent variable. $V_{b,n}$, $V_{T,n}$, $I_{o,n}$ and $R_{m,n}$ are roughly constant at a specified temperature, relative humidity and hydrogen flow rate. This equation applies only to the activation and ohmic regions, regions shown on the polarization curve (fig. 3). At currents that are high (around 2A for the cell used to show the curve), the fuel cell is limited by the rate of mass transfer to/from the electrode and the electrolyte. The model does not account for this limitation on current draw and the model falls apart. Since the model falls apart at high currents, a limitation was placed on the max range of currents that was used for regression. In addition, a minimum was placed on the range of currents used for regression, because they caused the the program used to regress (curve fit in python) to fail to converge to realistic numbers, returning battery voltages higher than the maximum theoretical output voltage at STP, with large confidence intervals of around 20 V. It is possible that the model has trouble predicting very low currents in the activation region, but further tests would need to be done to understand if this is the case.

A range of currents, 0.0684 A to 0.928 A, was regressed and returned reasonable results for cells 2, 3 and 4. Data for cell 1 appeared to have too much error to be properly regressed over the range of currents we examined. The results of the regression are shown below:

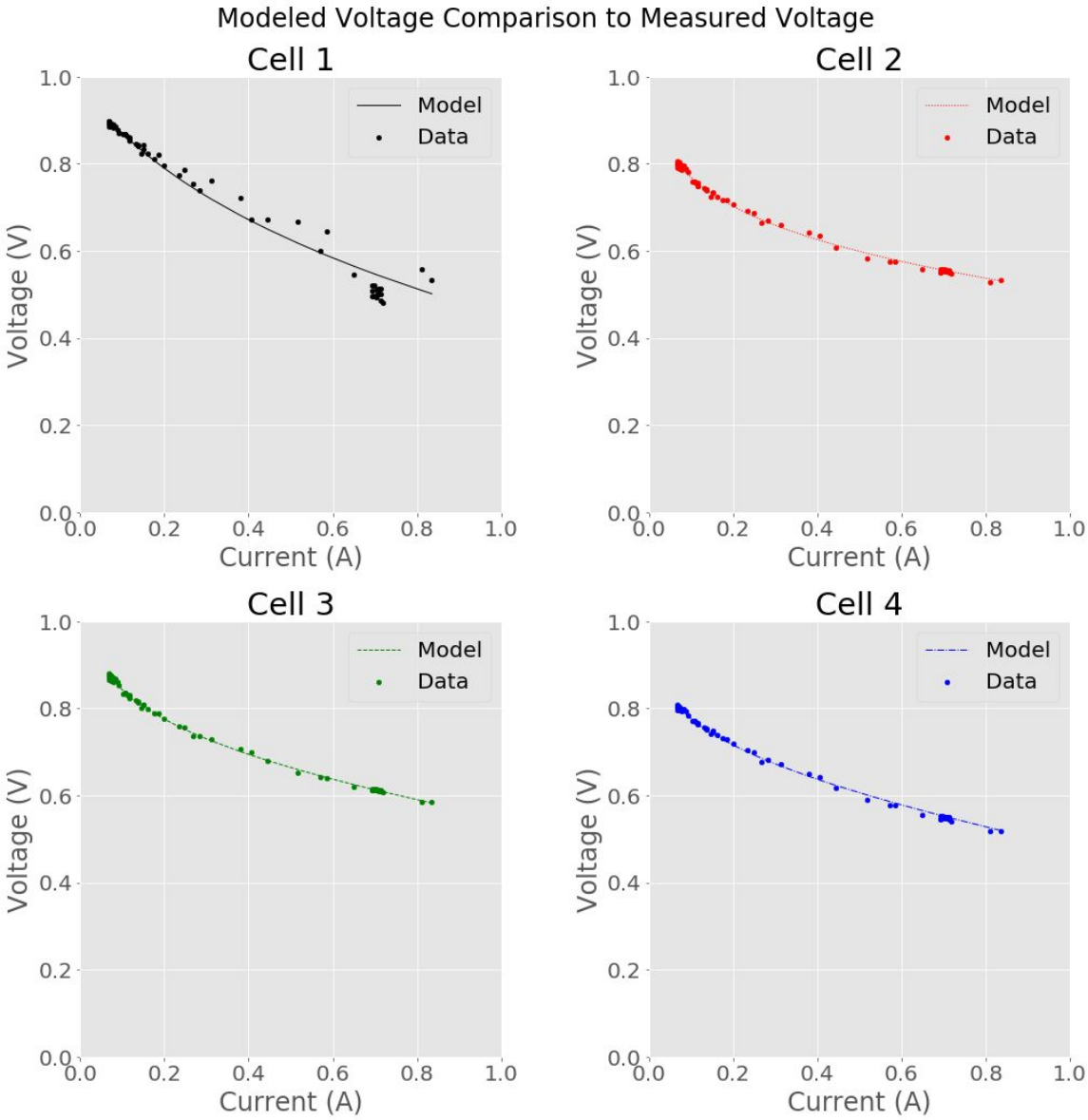

Fig 16. Modeled Voltage for Each Cell in Fuel Cell Stack

	Fit Parameters			
	Vb,n (V)	VT,n (V)	Io,n (A)	Rm,n (Ohms)
Cell 1	0.941	2729.250	85.025	-31.374
Cell 2	0.948	0.096	0.020	0.070
Cell 3	1.036	0.089	0.015	0.113
Cell 4	0.879	0.108	0.078	0.117

Table 1. Parameter Estimates for Regression

Confidence intervals were calculated from the covariance (an output of the curve fit python function), using the equation:

$$Conf = 1.96\sqrt{\sigma_{xx}}$$
$$\sigma_{xx} = Population\ Standard\ Deviation\ of\ x\ From\ Covariance\ Matrix$$
$$Conf = 95\%\ Confidence\ Interval$$

Eq. 4. 95% Confidence Interval Calculations

	Confidence Intervals			
	Vb,n (V)	VT,n (V)	Io,n (A)	Rm,n (Ohms)
Cell 1	0.0222	1.50E+06	2.34E+04	8.76E+03
Cell 2	0.1158	0.0379	0.0437	0.0646
Cell 3	0.1150	0.0262	0.0314	0.0458
Cell 4	0.0245	0.0554	0.0799	0.0742

Table 2. Confidence Intervals for Regression

The confidence intervals show that there is a large uncertainty in the saturation currents, but battery voltage was modeled with high confidence.

Mean square error (MSE) was also calculated as a comparison of the quality of each regression, with the MSE of the cell 1 regression being the highest (the farther from 0, the less accurate the regression).

$$MSE = \frac{\Sigma(\hat{y}_i - y_i)}{df}$$
$$MSE = Mean\ Square\ Error$$
$$\hat{y}_i = Modeled\ Data$$
$$y_i = Experimental\ Data$$
$$df = Degrees\ of\ Freedom = (\#tests) - (\#constants) = 60 - 4 = 56$$

Eq. 5. MSE equation.

In addition the Shapiro-Wilk test was used to analyze if the residuals of each regression followed a normal distribution (null hypothesis: population is normally distributed). It was found for cells 2, 3, and 4 that we cannot disprove that the residuals do not follow a normal distribution, since they have a high P-Value, but since the P-Value for the cell 1 regression was too low we can safely say that the residuals are not from a normal distribution.

	MSE	Shapiro-Wilk Test P-Value
Cell 1	5.14E-04	3.74E-07
Cell 2	2.73E-05	0.869622648
Cell 3	1.49E-05	0.711390376
Cell 4	1.63E-05	0.336676151

Table 3. MSE and Shapiro-Wilk Test P-Value

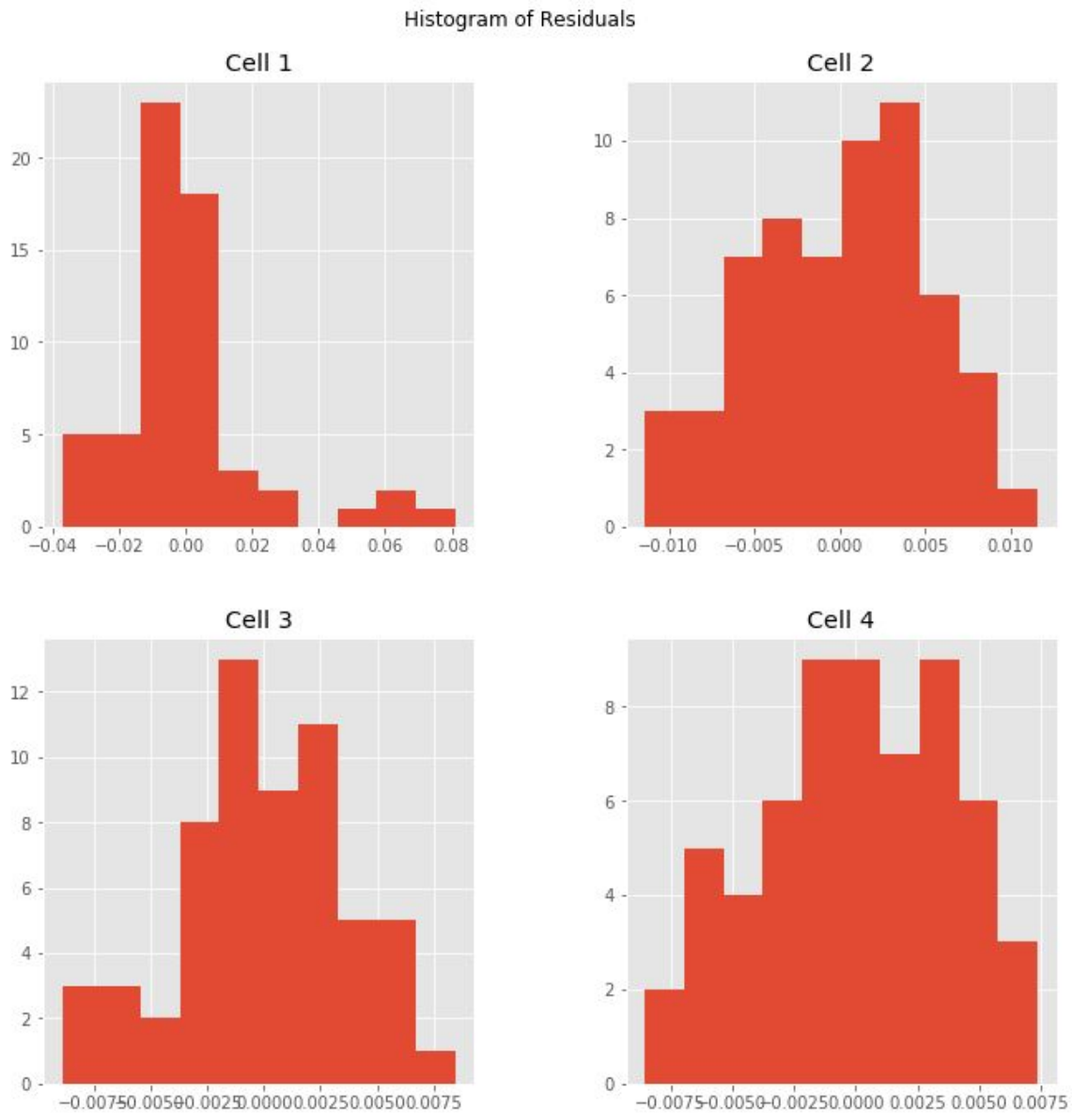

Fig 17. Histogram of Residuals Showing a Non-Normal Distribution in Cell 1 and Normal Distributions In the other cells.

The issues with cell 1 regression are very apparent when comparing current vs power curves. A modeled power curve was created by multiplying the equation for modeled voltage by current. The graphs generated from this method are pictured below:

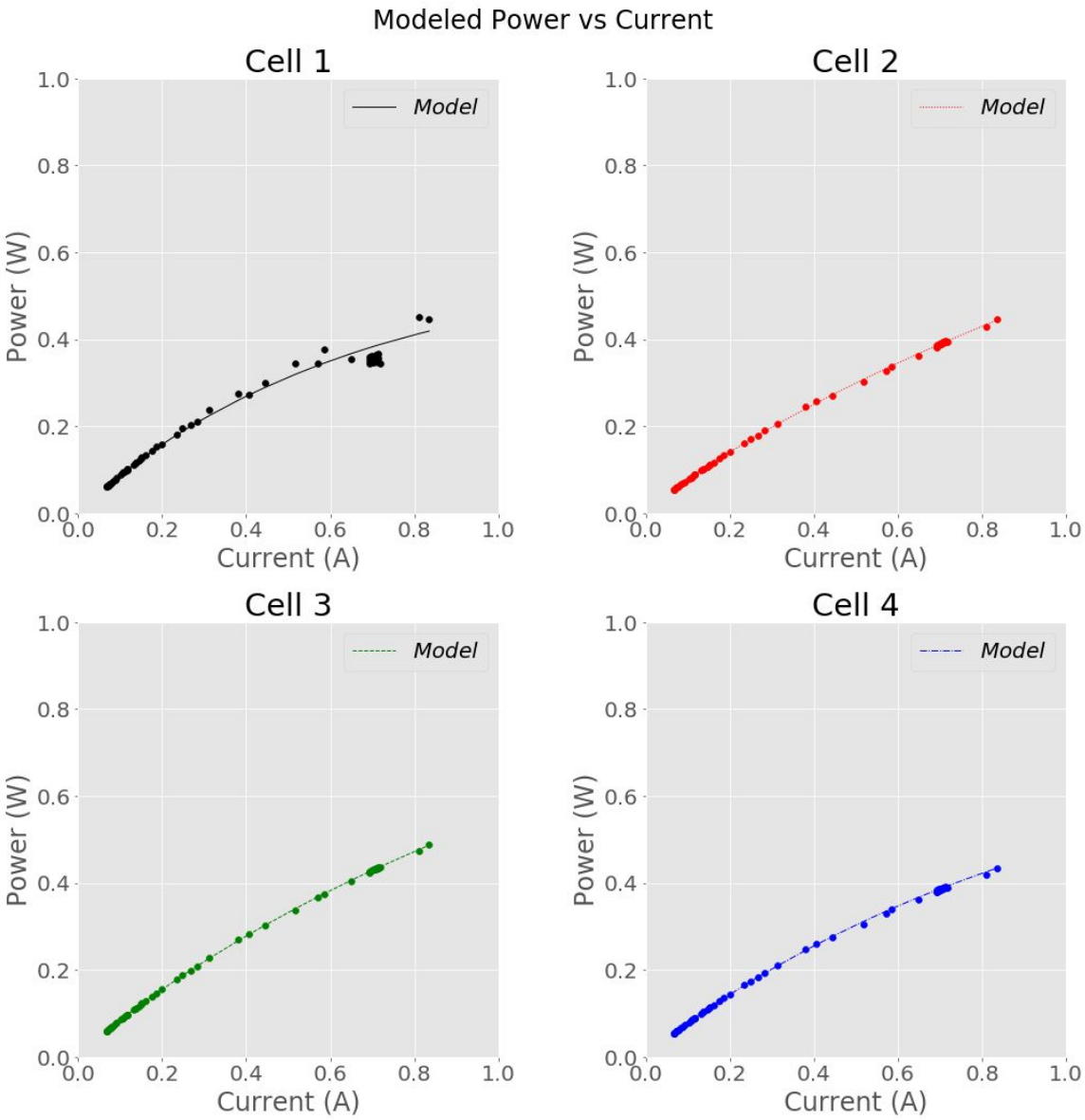

Fig 18. Modeled Power for Each Cell in Fuel Cell Stack

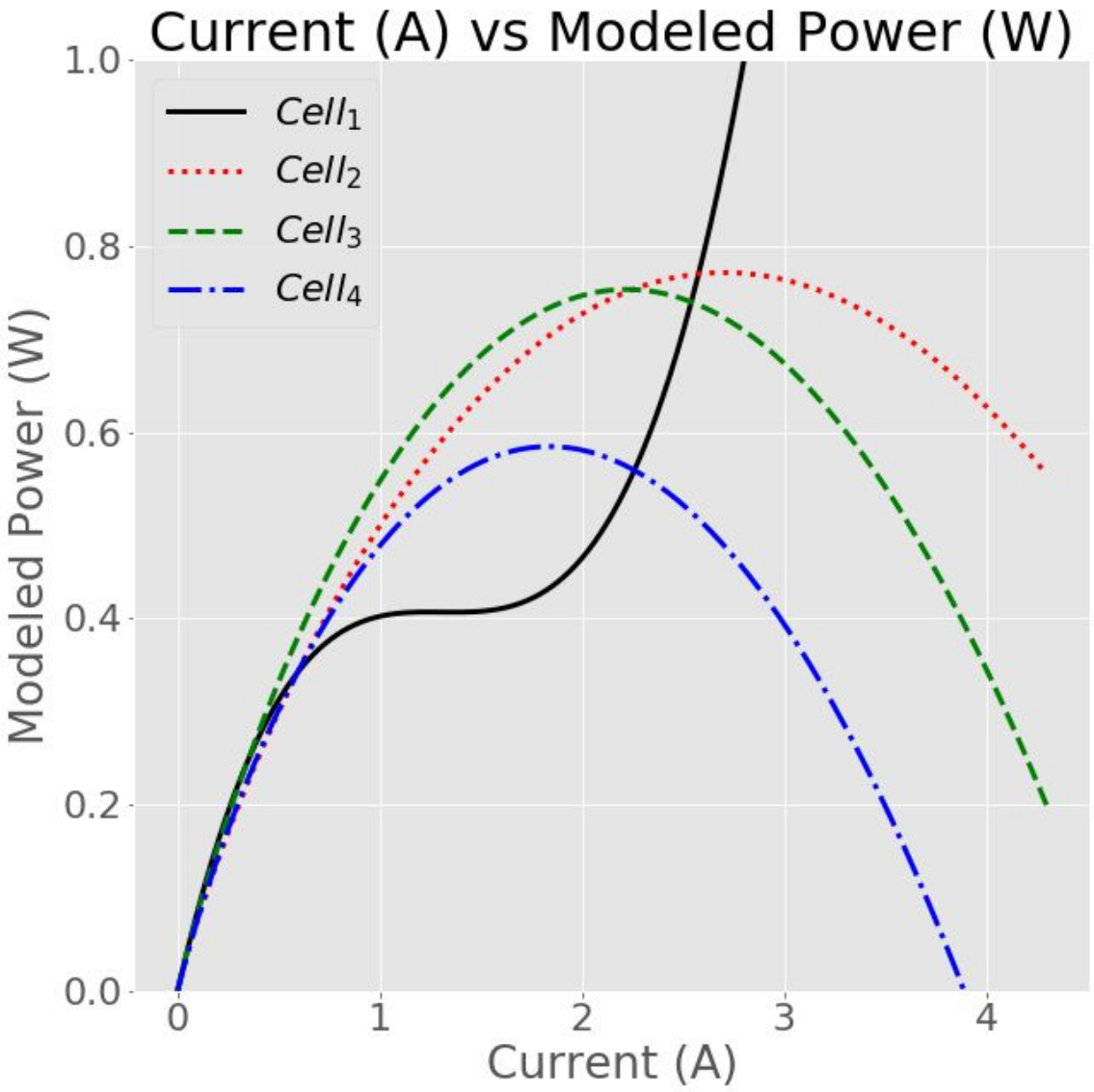

Fig 19. Modeled Power for Each Cell in Fuel Cell Stack

Additionally, if the power curve of each cell is extrapolated to higher currents, we can see that the regressed parameters for cell 1 completely fail to model the power curve that observed for the normal cells 2, 3, and 4.

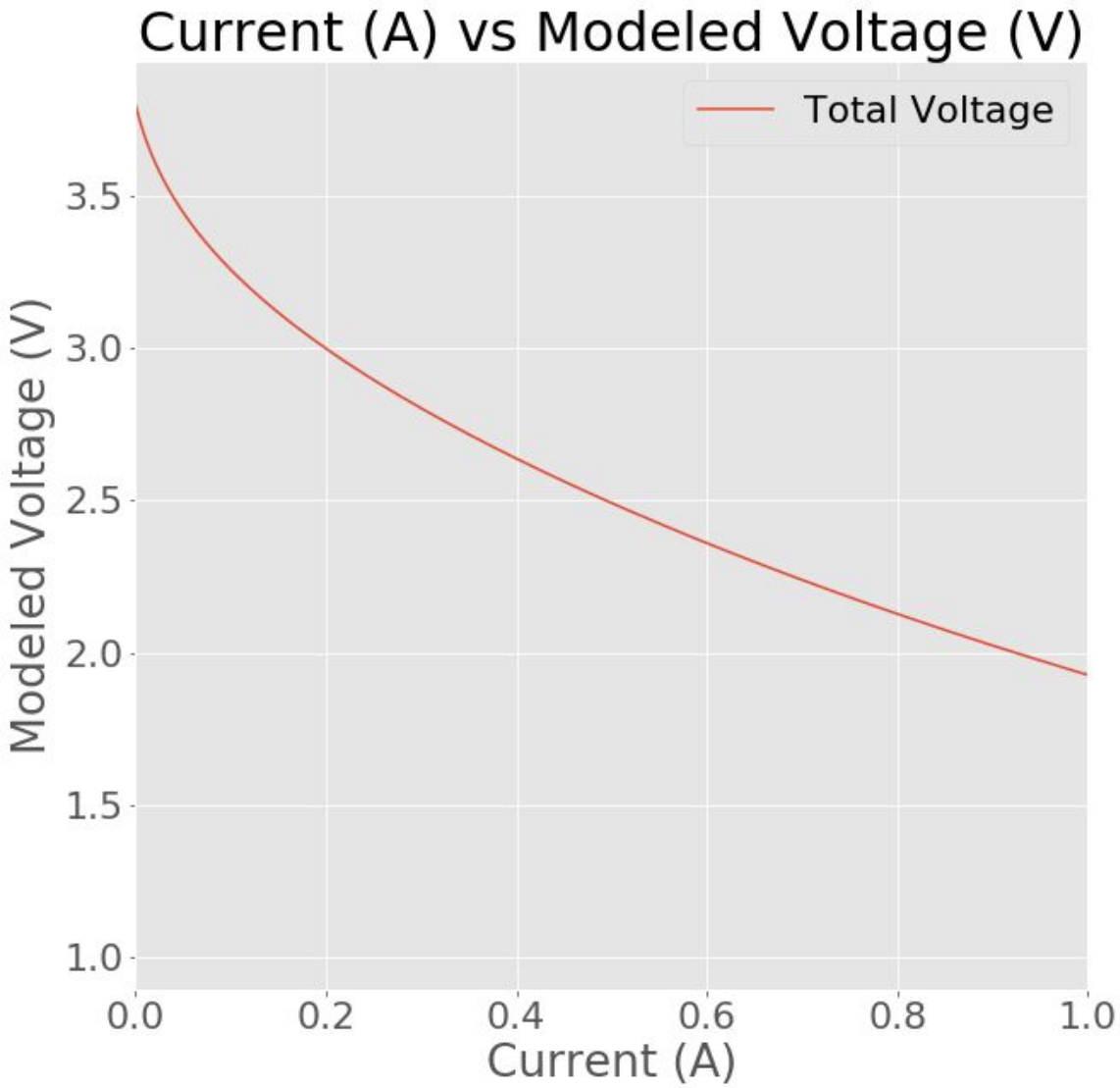

Fig 20. Modeled Total Voltage

However, at low currents, the model seems to predict the battery voltage with high confidence. The battery voltage is the max voltage that each cell can produce and we can add these to calculate the maximum efficiency of our whole system.

The maximum voltage, which occurs at current = 0 A is 3.8 V. Calculated from equation 2a multiplied by four to account for the number of cells in the stack the

theoretical V_{max}= 4.91 V, so efficiency$_{max}$ = 0.773. To compare, the theoretical maximum voltage for the perfect fuel cell is 94.5%, calculated using eq. 6. This is without any loss of heat where the only energy loss is from the difference between enthalpy and Gibbs Free energy. It is calculated as so.

$$\eta_{FC} = \frac{W_{OUT}}{Q_{IN}} = \frac{\Delta G_{Rxn}}{\Delta H_{Rxn}} = \frac{-228{,}588\,\frac{J}{mol}}{-\,241{,}818\,\frac{J}{mol}} = 94.5\%$$

Eq. 6. Theoretical Perfect Fuel Cell Maximum Efficiency[3]

The lack of clear data for cell 1 makes it hard to draw conclusions about the performance of the cell. For cells 2, 3, and 4 it appears that the internal resistance of the electrolyte changes in relation to the relative position of the cell in the stack. It is possible that the further down the stack a fuel cell is, the less optimal conditions occur for transport across the electrolyte. Flooding

Alternative Regression:

Because the fit for cell 1 was so poor the data was also regressed at a range of currents from 0.0684 A to around 1.94 A.. This broad range of currents (df = 130) returned a more reasonable regression for cell 1 than the previous regression, but returned worse Shapiro-Wilk P-Value for every other cell. Most of the residuals of the model fit are not normally distributed. For cell 2, where we cannot disprove that the fit is normal; this may be because cell two has not fully experienced the limits on the rate of reaction due to the limits of mass transfer. This may be because

in the range of current around 1.8 mass transfer is only limiting for those cells that are already poor, but for cell 2, which has less internal resistance in the electrode than the other cells, mass transfer is not fully limiting until higher currents.

	Fit Parameters			
	Vb,n (V)	VT,n (V)	Io,n (A)	Rm,n (Ohms)
Cell 1	0.979	0.270	0.213	0.059
Cell 2	0.939	0.107	0.027	0.045
Cell 3	1.055	0.088	0.011	0.110
Cell 4	0.932	0.077	0.019	0.144

Table 4. Parameter Estimates for Alternate Regression

	Confidence Intervals			
	Vb,n (V)	VT,n (V)	Io,n (A)	Rm,n (Ohms)
Cell 1	0.033	0.136	0.184	0.074
Cell 2	0.0475	0.0117	0.0203	0.0096
Cell 3	0.1118	0.0102	0.0191	0.0089
Cell 4	0.0683	0.0113	0.0260	0.0096

Table 5. Confidence Interval for Regression Alternate Regression

	MSE	Shapiro-Wilk P-Value
Cell 1	4.33E-04	1.62E-04
Cell 2	3.41E-05	0.06848
Cell 3	3.56E-05	0.01199
Cell 4	3.74E-05	0.00018

Table 6. MSE and Shapiro-Wilk Test P-Value for Alternate Regression

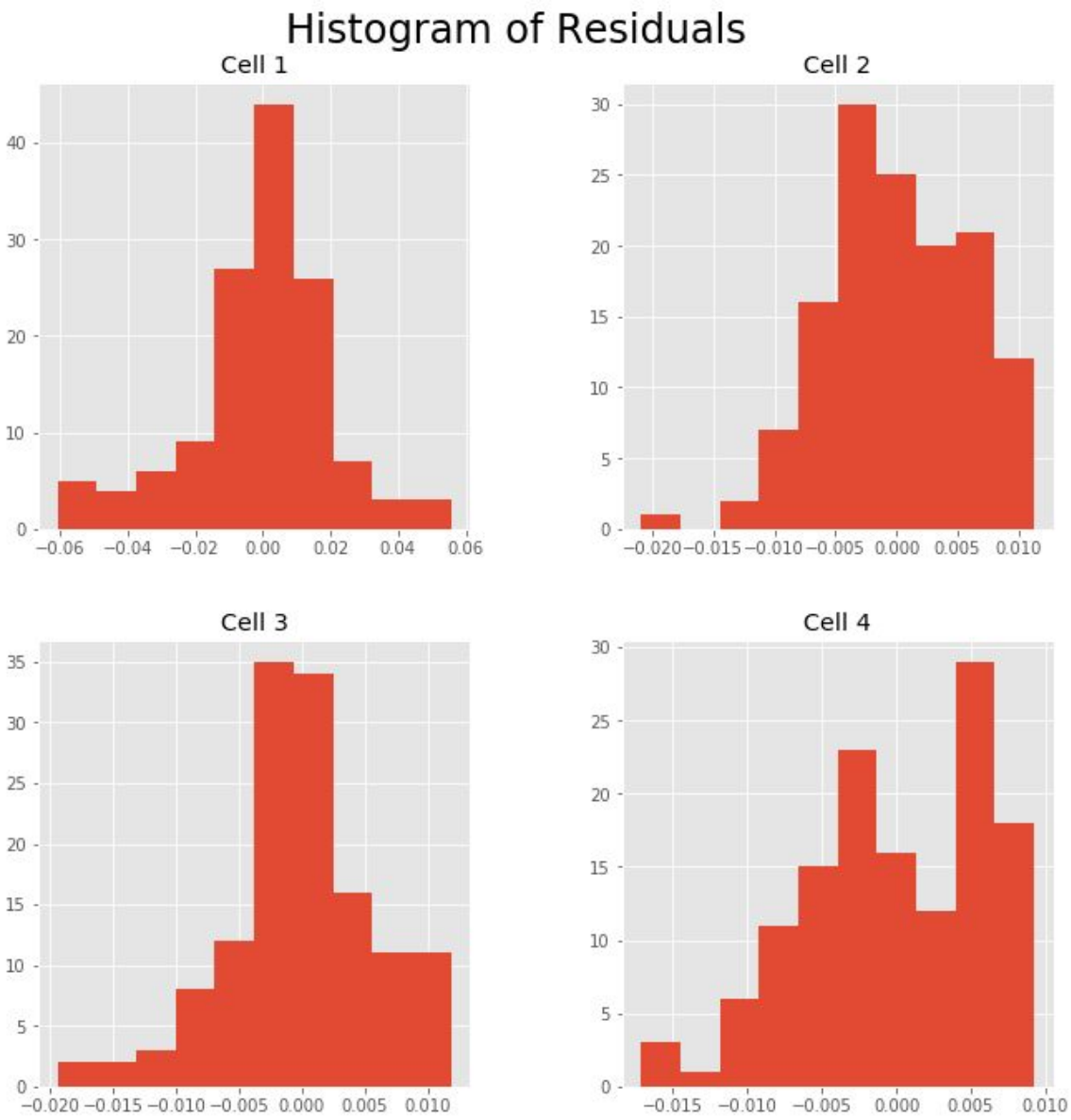

Fig 21. Histogram of Residuals For Alternate Regression Showing Non-Normal Distributions in most Cells

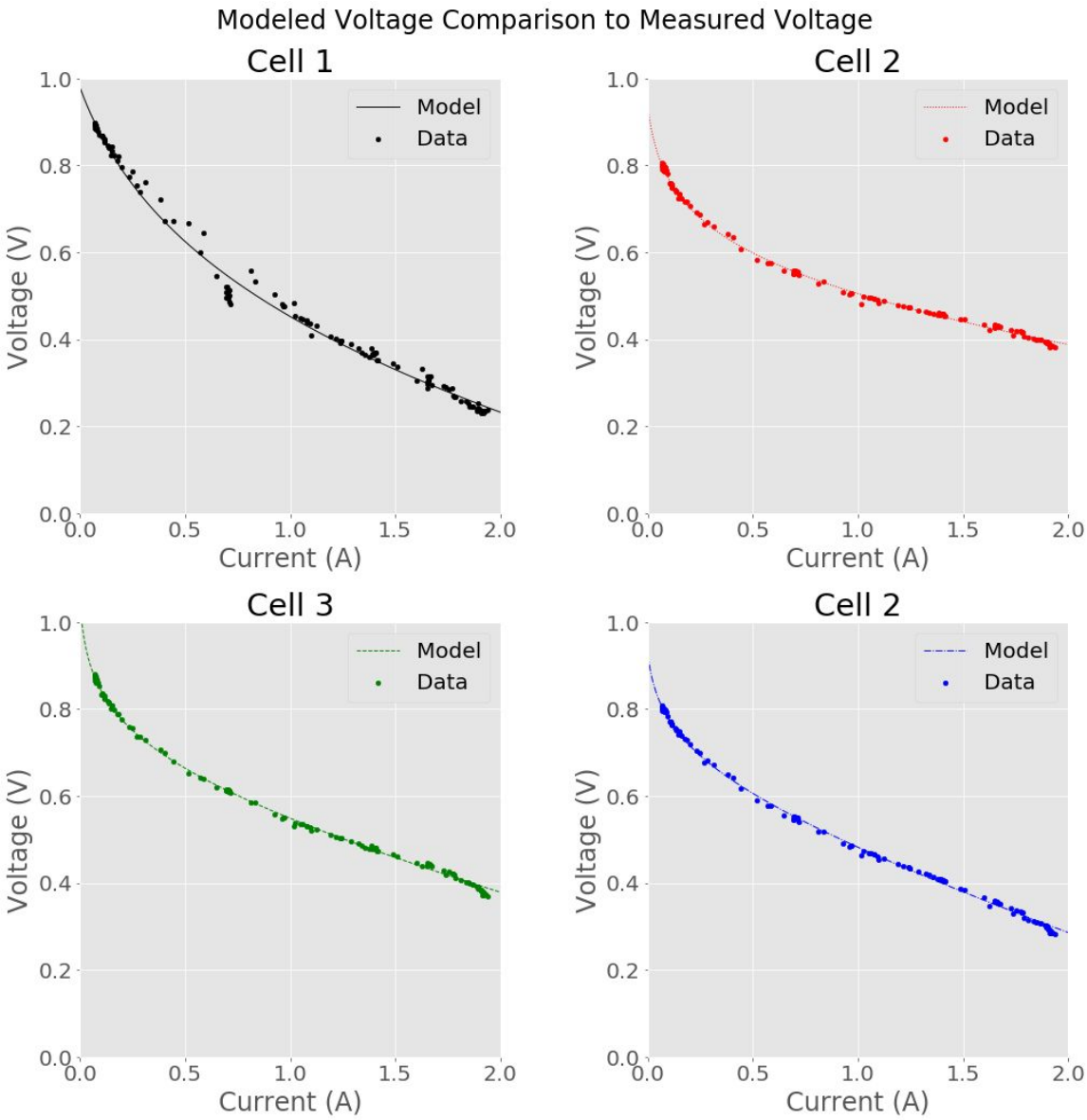

Fig 22. Modeled Voltage for Each Cell in Fuel Cell Stack for Alternate Regression

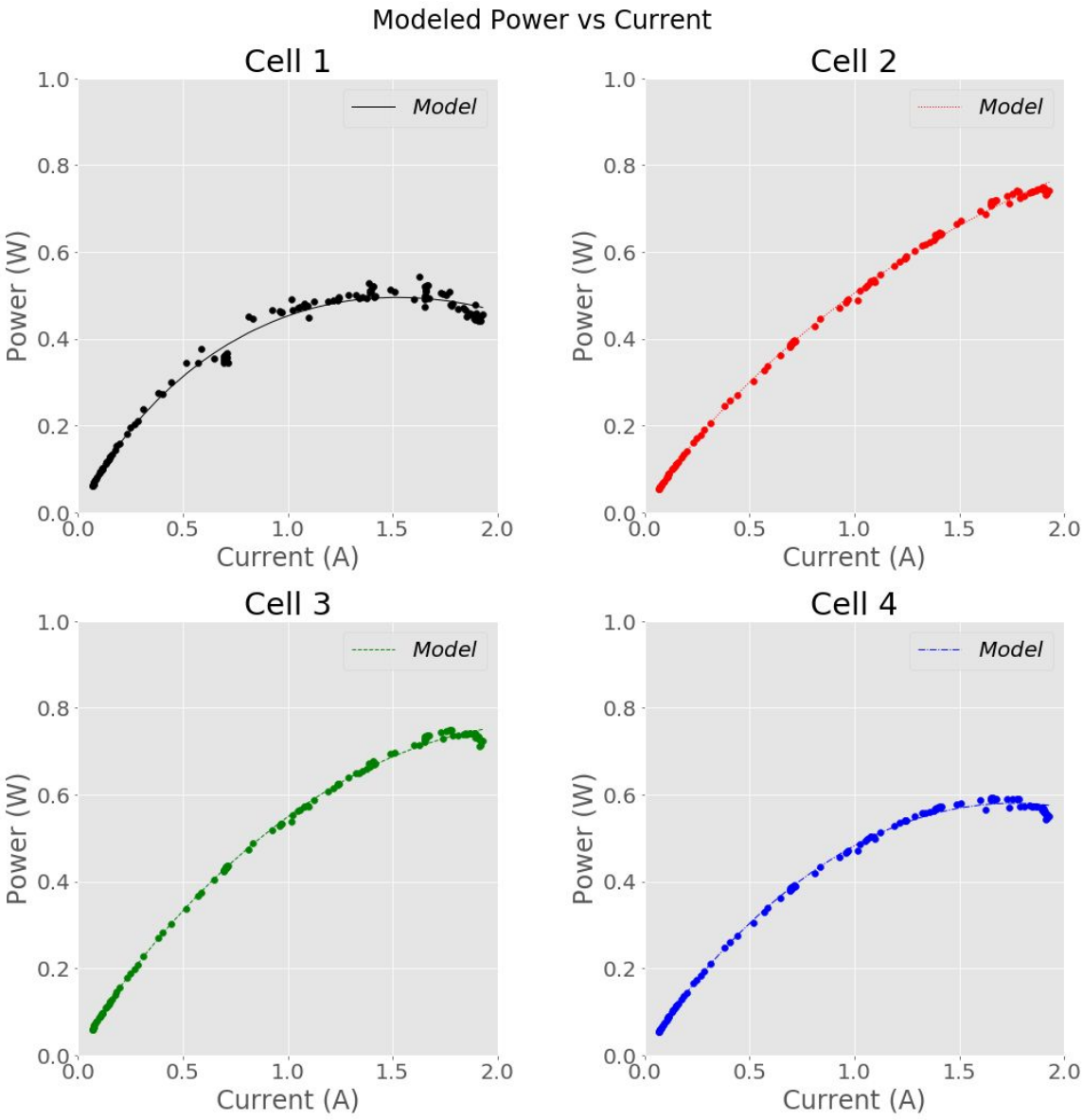

Fig. 23. Modeled Power for Each Cell in Fuel Cell Stack for Alternate Regression

While we cannot draw hard conclusions from these results there is a high threshold voltage and saturation current observed in cell 1 compared to other cells in the stack. The high values for these parameters can be caused by physical issues

with the electrodes/electrolyte contact in the fuel cell, such as delamination. More testing would have to be done to conclusively prove this.

As expected the model appears to hold somewhat true for the activation and ohmic regions of the polarization curve (Current Vs Voltage) and the power performance curve (Current Vs Power), but fails to model the mass transfer region, that begins around 1.8 A. The power and voltage sharply decrease around said voltage as shown by figures 22 and 23. While due to the non-random distribution in residuals the regression is not statistically sound, it appears to fit the data somewhat reasonably for each cell at low currents and at least provides a better fit for cell 1. Most likely, the alternate regression provides a better fit for cell 1 because the regression analysis includes more reasonable data points, which makes the noise from erroneous data points less impactful on the results of the regression.

If one were to use the models derived here, it would be recommended that the initial regression be used for cells 2, 3, and 4, and the alternate regression be used for cell 1, but only to model low currents. Both models, at the very least, are able to show which cells perform worse in terms of voltage and power output at low currents.

Error Analysis: Current Effects on Voltage and Failing Cells:

As mentioned before, when the unit was run at a constant load for a while, as current went higher, two of the fuel cells started to fail, as shown below.

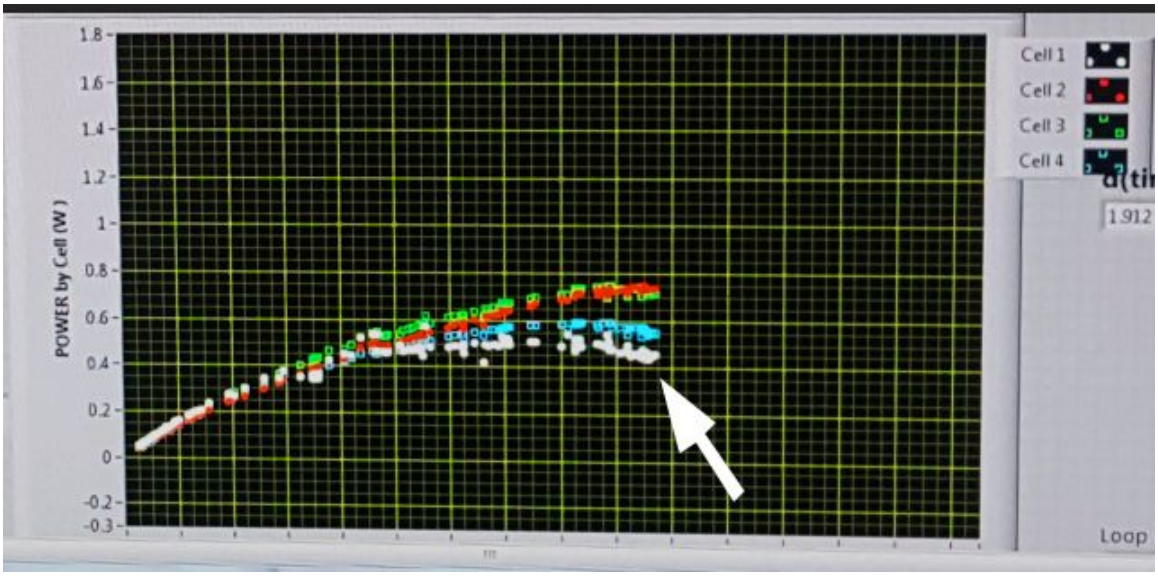

Current (A)

Fig. 15. Photo of LabView Program Running Indicating the Weakest Fuel Cell

This affected our humidity measurement. We carried out two series of measurements, both at constant load and temperature. In the first experiment we increased humidity from 30% to 60% and in the second we decreased humidity from 60% to 30%, recording the efficiency of our fuel cell stack. Logically, the curve going up and the curve going down should follow the same path if the fuel cells in the stack are unchanged.

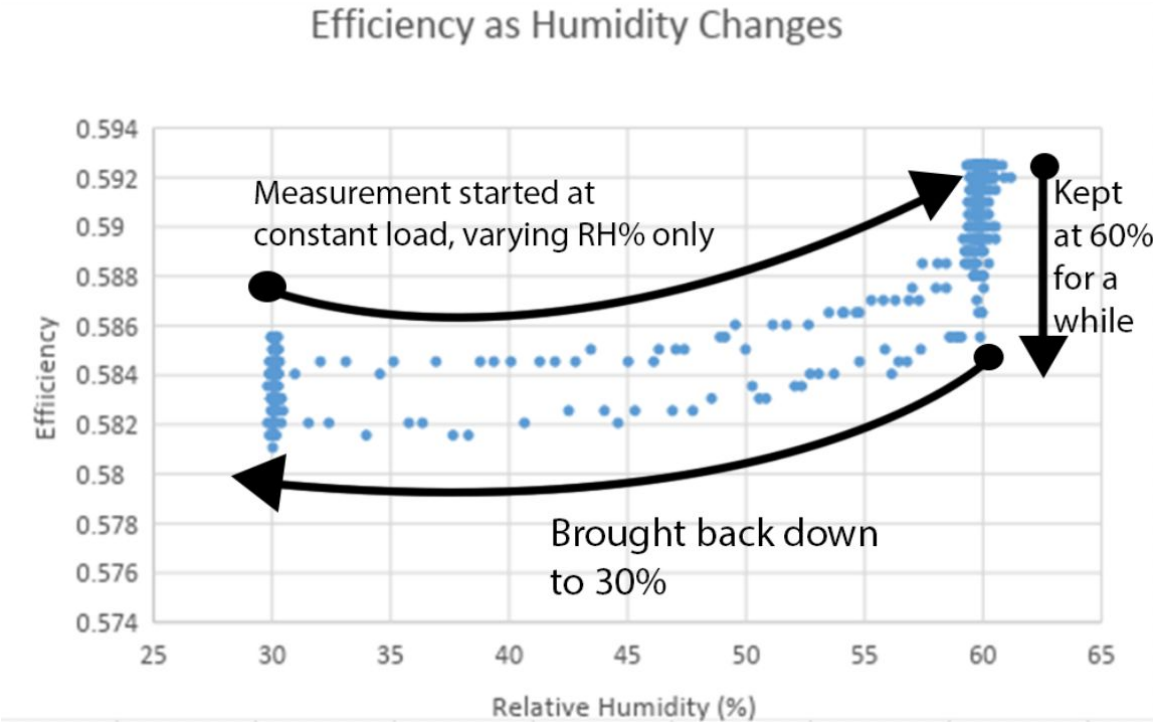

Fig. 25. Experimental Data Indicating Drop in Total Fuel Cell Performance over Time

However, as observed in figure 25, there are two distinct curves, with the second curve (60% to 30%) having an overall lower efficiency. This means that one of the cells in the stack must have changed between runs. Two cells, the first cell (white) and the last cell (blue) were observed to have decreased voltages while they were held at constant loads. The same issue was not observed when using a square wave, where external resistance was varied from a high value of around 92 ohms to the desired resistance at a lower external resistance. When there is a high external resistance applied to the fuel cell stack, the current draw is minimal, so the cells may be able to "rest", meaning that when a higher current is needed, the cell is able to operate at a reasonable, consistent capacity. This is why all of runs carried out after

this one either had a short duration at a constant load or a long duration run entirely with a square wave.

One explanation for cells 1 and 4 being weaker could be because they were exposed to the elements more than the other two. The cells that failed were on the outside of the stack, so they may be most likely to suffer structural damage. Alternatively, cells that performed worse could have done so because of their internal elements, like their internal resistance being higher than the other cells.

A source of error that was mentioned before was that changing temperature was hard to do in complete isolation. Within the fuel cell box, a change in temperature would be likely to change humidity, due to the higher water temperature making more evaporation possible. In the system we used, it is hard to make humidity completely independent of temperature change.

Another source of error could come from the measuring equipment used. Determining and measuring the exact outputs given using the LabJacks could have inherent error because of the equipment and sensor designs. For example, the temperature sensor used was a TMP37 which has an accuracy of $\mp 2°C$, which means that some of the temperature measurements could have been slightly off.

Limitations:

Fan speed was taken from 99% to 0%, to see if there was an effect on the fuel cells. This shift caused the voltage of some fuel cells to become negative, so the speed was promptly taken back up to 100%. Fan speed may have an effect on fuel cell efficiency and power, but for the sake of the integrity of our system we chose not to test fan speed.

Temperature was also a limitation because we were only able to measure within a 35 degree range. It would have been beneficial to measure the effects on power and efficiency for temperatures beyond 60°C. Electrochemical energy appears to decrease for a reversible cell at temperatures above 400 K (Pilatowsky 2011), so seeing the effects on the fuel cell that we had would be quite interesting.

Conclusion:

Our findings conclude that it is impossible to maximize both power and efficiency. As one is increased, the other dips in the manner modeled by the power-performance curve. However, to maximize either one is very much possible. The maximum efficiency occurs at a low current (thermodynamically, at a current of zero), and for our system would theoretically be 82.8%, with an accompanying voltage of 4.91 V, and low power and resistance. The maximum power would occur at a current of 2.01 A and would be 2.56 W. Power, efficiency, and voltage can be affected by humidity and temperature as when both increase, the power, efficiency and voltage increase alongside them.

References:

[1] Benziger, Jay B., et al. "The Power Performance Curve for Engineering Analysis of Fuel Cells." *Journal of Power Sources*, vol. 155, no. 2, 16 Mar. 2005, pp. 272–285., doi:10.1016/j.jpowsour.2005.05.049.

[2] Dowdall, Libby. "Molecular Fuel Cell Catalysts Hold Promise for Efficient Energy Storage."*News*, University of Wisconsin-Madison, 15 July 2015, https://news.wisc.edu/molecular-fuel-cell-catalysts-hold-promise-for-efficient-energy-storage/ .

[3] Lutz, Andrew E., et al. "Thermodynamic Comparison of Fuel Cells to the Carnot Cycle."*International Journal of Hydrogen Energy*, Pergamon, 18 Mar. 2002, www.sciencedirect.com/science/article/pii/S0360319902000162 .

[4] Pilatowsky I., Romero R., Isaza C., Gamboa S., Sebastian P., Rivera W. (2011) Thermodynamics of Fuel Cells. In: Cogeneration Fuel Cell-Sorption Air Conditioning Systems. Green Energy and Technology. Springer, London.

[5] Smith, J. M., et al. *Introduction to Chemical Engineering Thermodynamics*. 8th ed., McGraw-Hill Education, 20 Mar. 2017.

[6] Yeetsorn, Rungsima, et al. "A Review of Thermoplastic Composites for Bipolar Plate Materials in PEM Fuel Cells." *Nanocomposites with Unique Properties and Applications in Medicine and Industry*, 2011, doi:10.5772/19262.